Water Research X 18 (2023) 100178

Contents lists available at ScienceDirect

Water Research X

journal homepage: www.sciencedirect.com/journal/water-research-x

Gravity-driven membrane filtration with compact second-life modules daily backwashed: An alternative to conventional ultrafiltration for centralized facilities

Deborah Stoffel [a], Nicolas Derlon [a], Jacqueline Traber [a], Christian Staaks [b], Martin Heijnen [b], Eberhard Morgenroth [a,c], Céline Jacquin [a,*]

[a] Eawag, Swiss Federal Institute of Aquatic Science and Technology, Überlandstrasse 133, Dübendorf 8600, Switzerland
[b] inge-DuPont, Flurstraße 27, Greifenberg 86926, Germany
[c] ETH Zürich, Institute of Environmental Engineering, Zürich 8093, Switzerland

ARTICLE INFO

Keywords:
Gravity-driven membrane filtration
Ultrafiltration
Backwash frequency
Second-life membranes
Centralized systems
Energy costs

ABSTRACT

Gravity-driven membrane (GDM) filtration is a strategic alternative to conventional ultrafiltration (UF) for the resilient production of drinking water via ultrafiltration when resources become scarce, given the low dependency on energy and chemicals, and longer membrane lifetime. Implementation at large scale requires the use of compact and low-cost membrane modules with high biopolymer removal capacity. We therefore evaluated (1) to what extent stable flux can be obtained with compact membrane modules, i.e., inside-out hollow fiber membranes, and frequent gravity-driven backwash, (2) whether we can reduce membrane expenses by effectively utilizing second-life UF modules, i.e., modules that have been discarded by treatment plant operators because they are no longer under warranty, (3) if biopolymer removal could be maintained when applying a frequent backwash and with second-life modules and (4) which GDM filtration scenarios are economically viable compared to conventional UF, when considering the influence of new or second-life modules, membrane lifetime, stable flux value and energy pricing. Our findings showed that it was possible to maintain stable fluxes around 10 L/m^2/h with both new and second-life modules for 142 days, but a daily gravity-driven backwash was necessary and sufficient to compensate the continuous flux drop observed with compact modules. In addition, the backwash did not affect the biopolymer removal. Costs calculations revealed two significant findings: (1) using second-life modules made GDM filtration membrane investment less expensive than conventional UF, despite the higher module requirements for GDM filtration and (2) overall costs of GDM filtration with a gravity-driven backwash were unaffected by energy prices rise, while conventional UF costs rose significantly. The later increased the number of economically viable GDM filtration scenarios, including scenarios with new modules. In summary, we proposed an approach that could make GDM filtration in centralized facilities feasible and increase the range of UF operating conditions to better adapt to increasing environmental and societal constraints.

1. Introduction

In a context of energy constraints and issues with chemical or membrane supply, the implementation of gravity-driven membrane (GDM) filtration as an alternative to conventional ultrafiltration (UF) is particularly relevant. Conventional UF consumes 0.01–0.07 kWh/m^3, representing considerable annual costs for a treatment plants when UF is the main treatment, especially given the current rise in energy prices (Hawari et al., 2020; Santos et al., 2021). Also, in a context of electricity shortage, the energy requirements for conventional UF could constraint drinking water production (Mišík, 2022). Instead, GDM filtration eliminates the need for filtration pumps and chemicals and extends membrane lifetime, significantly reducing filtration energy-demand and securing operation in the event of resource scarcity (Pronk et al., 2019). However, GDM filtration is still regarded as an approach only relevant for decentralized facilities due to: (1) the low compactness of GDM systems, which are frequently implemented with flat sheet modules or outside-in hollow fiber (HF) modules with low packing density, and (2)

* Corresponding author.
E-mail address: celine.jacquin@eawag.ch (C. Jacquin).

https://doi.org/10.1016/j.wroa.2023.100178

Available online 29 March 2023

low steady flux values, resulting in higher membrane investment costs compared to conventional UF (Pronk et al., 2019; Stoffel et al., 2022). Investigating how to achieve high flux values with compact membrane geometry modules, while identifying a suitable approach to make the process economically viable compared to conventional UF, is crucial to move toward the implementation of GDM filtration at centralized facilities.

Applying GDM filtration with highly compact membrane modules results in a significant flux reduction, making the process irrelevant for centralized facilities (Stoffel et al., 2022). For instance, flux was reduced from 15.2 to 8.5 L/m^2/h when increasing the packing density of modules with outside-in HF membranes from 352 m^2/m^3 to 2151 m^2/m^3 (Wu et al., 2017). In another study, highly compact spiral wound reverse osmosis (RO) modules that had undergone chemical conversion into UF-like modules had a flux of 1.5 L/m^2/h when filtering deionized water at a transmembrane pressure (TMP) of 0.16 bar (García-Pacheco et al., 2021). This stable flux value is insufficient for centralized facilities. Furthermore, the filtration tests conducted by García-Pacheco et al. (2021) may not be long enough to estimate the real stable flux of spiral wound modules operated in GDM filtration. The tests only lasted 360 min, while the characteristic time to reach a stable flux during GDM filtration is usually of 5–7 days (Pronk et al., 2019). Additionally, spiral wounded modules are rather compact in design (membrane layers are separated by a distance of about 1 mm), and even after 5 days of operation, the flux will likely continue to decline. Indeed, in a recent work, we showed that for modules equipped with inside-out HF having an inner diameter of 0.9 mm and operated with relaxation and forward flush, the flux constantly decreased at a rate of 0.16 L/m^2/h/d during the 125 days of the experiment and the final flux was between 0 and 2 L/m^2/h (Stoffel et al., 2022). By applying a one-time gravity-driven backwash, we were however able to temporarily increase the flux and therefore suggested intermittent backwash might be effective to operate GDM systems with inside-out HF membranes at a stable flux. Nonetheless, it is yet unknown if frequent backwash can successfully balance the continuous flux decline observed for compact membrane modules such as for modules with inside-out HF membranes.

If membranes with more compact geometries can be successfully operated at a high stable flux for GDM filtration (around 10 L/m^2/h), such flux will remain significantly smaller than the flux of conventional UF in centralized facilities. The rise in membrane investment costs would have severe adverse economic effects on the drinking water treatment plant (Pronk et al., 2019). A relevant strategy to lower membrane investment costs is to refurbished UF modules. Refurbishing modules is being researched in the context of conventional UF, but using RO and nanofiltration modules chemically converted into UF-like modules (Lawler et al., 2013; Senán-Salinas et al., 2019). The use of recycled spiral wound RO modules for GDM filtration did, however, result in low flux values, as previously discussed (García-Pacheco et al., 2021). Therefore, refurbished RO and nanofiltration modules would be difficult to use for GDM filtration in centralized facilities. Using decommissioned UF modules recovered from the drinking water industry that passed the membrane integrity test, or second-life modules, is an unexplored possibility to lower the membrane investment costs of GDM filtration. The UF modules are frequently discarded not because of any notable problems with their integrity, but mainly because they have reached the end of their warranty period or because their permeability has decreased. Consequently, discarded UF modules represent a significant resource of good quality modules for recycling. The question that this innovative approach poses is whether or not membrane aging results in lower fluxes than new membranes when used in GDM filtration mode, because initial permeability could be reduced (Robinson et al., 2016).

It is essential to ensure that performing repeated backwashes and employing second-life modules do not adversely affect the biopolymer removal compared to GDM filtration with no maintenance and new modules, as it is a main asset of GDM filtration (Ranieri et al., 2023). Biopolymer retention is partly due to the membrane retention; in GDM filtration between 20 and 40% of the biopolymers are removed by the membrane (Stoffel et al., 2022). However, major part of the removal is due to the biofilm establishment at the surface of the membrane (Derlon et al., 2014; Pronk et al., 2019). The biofilm acts as a secondary biologically-active barrier that can better retain and biodegrade biopolymers (Chomiak et al., 2015; Park et al., 2016). The enhanced biopolymer removal reported for in presence of biofilm compared to virgin membrane therefore helps improving the permeate biological stability. Such enhanced biopolymer removal by GDM systems also has the potential to increase the efficiency of post-treatment such as reverse osmosis or photocatalysis, as biopolymers are major membrane foulants and phototacalysis quenchers (Akhondi et al., 2015; Maghsoodi et al., 2019; Yin et al., 2020). From one hand, applying a frequent backwash could affect the biofilm thickness and membrane coverage. Biofilm instability brought by the backwash has been observed with optical coherence tomography (OCT) by Shao et al. (2018). OCT images showed exposed virgin membrane, or areas deprived of a biofilm, which may lead to lower biopolymer removal following backwash. In contrast, Wu et al. (2019) found no relationship between the length of the backwash and the removal of the biopolymers. Therefore, it is unknown how a regular backwash might impact GDM filtration's ability to remove biopolymers. On the other hand, it is unclear if biopolymer removal would be adversely impacted by the usage of second-life modules, as extensive chemical cleaning of conventional UF modules could result in decreased dissolved organic removal compared to new membrane due to membrane aging, which manifests through material elongation, pore expansion, and the occurrence of breaches (Regula et al., 2014). In definitive it is crucial to further research on the potential impacts of these maintenance and cost reduction practices on GDM filtration's ability to remove biopolymers.

The main purpose of this study was to evaluate how to tackle the main challenges associated with the implementation of GDM filtration in centralized drinking water facilities: (1) maintain a stable flux with membranes having a compact geometry, (2) decrease membrane investment costs and (3) ensure high biopolymer removal. For this purpose, we first investigated the effect of gravity-driven backwash frequency on the flux of modules equipped with 7-capillaries inside-out hollow fiber (HF) membranes having an inner diameter of 0.9 mm. To reduce membrane investment costs of GDM filtration, we examined whether second-life membranes performed similarly to new membranes using the optimal backwash frequency identified based on filtration flux values. In addition to flux measurements, we assessed the impact of backwash frequency and module type on the permeate quality when measuring the removal of biopolymers. Afterwards, we compared the costs of conventional UF, GDM filtration with new membranes, and GDM filtration with second-life membranes in various scenarios. More particularly, we calculated the membrane investment costs and the operating expenditures (OPEX) corresponding to energy requirements and chemical cleaning considering several factors: membrane types, membrane lifetime, stable flux, and energy prices.

2. Material and methods

2.1. New and second-life UF modules characteristics

Modules equipped with 0.9 mm Multibore™ membranes from Dupont were used in this study (Table 1). Multibore™ membranes are modified polyether sulfone (PES) hollow fiber membranes with a pore size of 20 nm. One fiber consists of seven separate capillaries with an inner capillary diameter of 0.9 mm. We prepared two types of lab-scale modules containing 0.9 mm 7-capillaries HF membranes in a polyvinyl chloride (PVC) shelf for our experiments: (1) modules equipped with new membranes and (2) modules equipped with second-life membranes collected from a dizzer XL 0.9 MB 80 WT module taken from a drinking water treatment, which is not named here for privacy concerns

Table 1
Membrane module types used in this study and their main characterizations.

Parameter	Module type 1	Module type 2
Module length [cm]	140	140
Number of fibers per module	10	8
Internal capillary diameter [mm]	0.9	0.9
Membrane surface area [m^2]	0.22	0.20
Previous module operation time [year]	0 (new)	5 (second-life)
Permeability [L/m^2/h/bar]	574.2 ± 29.4	466.2 ± 80.1

We characterized the inside and outside of new and second-life membrane surface with scanning electron microscopy (SEM) using a Zeiss Gemini 460 FEG (Germany). Dry membranes have been coated with 5 nm of gold and we used a magnification of 10,000 and a beam accelerating voltage of 1 kV.

(Table 1). The dizzer XL 0.9 MB 80 WT module had been in operation for five years to treat reservoir water and was replaced because its warranty had expired. To ensure reproducibility of the experiment, we chemically cleaned the second-life modules before use, following the procedure described in supplementary data (section 1).

2.2. Experimental set-up

The experimental set-up is described in Fig. 1. The feed water was river water pumped from the river Chriesbach (Dübendorf Switzerland) into a sedimentation tank with a volume and a residence time of 155 L and 100 min, respectively. The supernatant of the sedimentation tank flowed into the raw water channel (volume of 240 L). The raw water channel level was adjusted to 80 cm to reach an average TMP of 150 mbar, given that modules are 140 cm long, as chosen previously (Stoffel et al., 2022).

Table 2 presents the characteristics of the raw water after the sedimentation tank. The inflow and outflow pipes of the installed modules were equipped with magnetic 3-way valves connected to timers to apply programmed maintenances. Since the backwash was conducted with permeate, the produced permeate was collected and pumped to the backwash channel (volume of 80 L). The water level of the backwash tank was set to 280 cm to reach an average TMP of 350 mbar, given that modules are 140 cm long.

Table 2
Influent characteristics after the sedimentation tank.

Characteristics	Mean ± standard deviation
Temperature [°C]	16.7 ± 1.9
Turbidity [NTU]	2.3 ± 1.9
Mean particle size [μm]	49 ± 31
Dissolved organic carbon (DOC) [mg/L]	1.9 ± 0.5
Biopolymer concentration [μg/L]	56.1 ± 19.0

2.3. Operating strategies

Different backwash frequencies were studied: (i) no backwash (nBW), (ii) backwash every two weeks (2wBW), (iii) weekly backwash (wBW) and (iv) daily backwash (dBW). The backwash procedure was established based on previous study and consisted of two sequential backflushes with a water head of 280 cm with a 1 min break in between (Stoffel et al., 2022). Each backflush lasted 2 min to ensure a sufficient flushing of the biofilm debris. During the first minute of the backflush, the upper backwash line was opened to remove particulate matter accumulated on top of the module. During the second minute, the lower backwash line was additionally opened. Based on the results from our previous study, we also applied a daily relaxation (55 min) followed by a forward flush (5 min) (*R*+FF) to all modules (Oka et al., 2017; Stoffel et al., 2022).

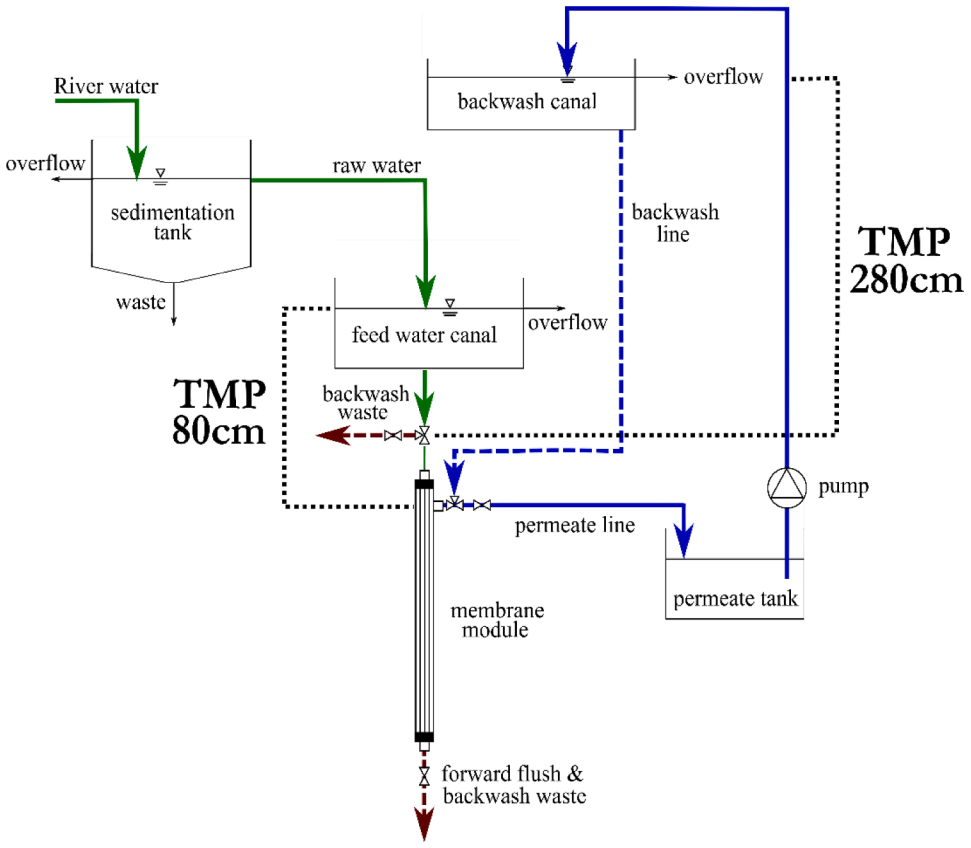

Fig. 1. GDM filtration experimental set-up. The green, blue, and black solid lines represent the feed water, permeate and tank overflow/drainage, respectively. The blue and brown dotted lines represent the backwash and wastewater of the different types of maintenances (forward flush or backwash), respectively.

2.4. Backwash with increased pressures at the end of the experiment

We designed a one-time backwash experiment to determine whether higher biofilm removal resulted in a lower biopolymer elimination on the short-term, using the backwash procedure described in section 2.3.1. The experiment was conducted on dBW1_new, 2wBW1_new and dBW1_SL at day 142. It consisted in three sequential backwash procedures at different TMP (350, 400 and 600 mbar). The backwash at 350 mbar was gravity-driven and we used a pump to apply a TMP of 400 and 600 mbar. The TSS collected during each backflush were measured as indicator of biofilm removal. After each backwash procedure, we waited three hydraulic retention times (HRT) of each module to sample raw water and permeate and measured their respective biopolymer concentrations (calculations explanations in section 2 of supplementary data). For this experiment, we enriched the river water in the feed water canal with secondary effluent of the wastewater treatment plant of Eawag (Dübendorf, Switzerland) to enhance the biopolymer concentration and increase the removal calculation accuracy given the LC—OCD detection limit. During the experiment, the dissolved organic carbon and biopolymer concentrations in the feed water tank were equal to 3.5 mgC/L and 222 µg/L, respectively. All experiments and maintenances applied in the current study are listed in Table 3.

2.5. Measurements and calculations

Daily flux measurements were taken to evaluate the productivity of each module. The produced permeate was collected twice a day for 3 h (before and after the maintenance) and weighted on a scale. The flux was calculated using the Darcy law and normalized at 20 °C using the temperature in the raw water channel measured with a portable device (WTW, Multi 3630 IDS SET KS2 Field Case w/o Sensor).

TSS amount in backflush water was used as an indicator for biofilm removal during the backwash procedure as in situ observation of the biofilm in the lumen was not possible without module sacrifice. The TSS were measured once per week for one module per backwash frequency and module type using the APHA standard method (APHA, 2005).

Every two weeks, we monitored influent and permeate quality for one module per frequency and module type, using liquid chromatography coupled with organic carbon detection (LC—OCD) to quantify the biopolymer removal. This method separates the dissolved organic carbon into five different fractions and quantifies them, i.e., biopolymers (> 20 kDa), humics (1 – 2 kDa), building blocks (0.5 – 1 kDa), low molecular weight organic acids and neutrals (0.35 – 0.5 kDa). The separation is based on the molecular size and occurs in the chromatographic column (Monnot et al., 2016). More details on the instrument and method are available elsewhere (Huber et al., 2011; Jacquin et al., 2020). The samples were taken around 2 h after the maintenance.

Table 3
Summary of the modules and maintenance strategies.

Module type	Module name *	Backwash frequency	Backwash at higher pressures
New	dBW1_new	daily	one-time experiment
	dBW2_new	daily	–
	wBW1_new	weekly	–
	wBW2_new	weekly	–
	2wBW1_new	every two weeks	one-time experiment
	2wBW2_new	every two weeks	–
	nBW1_new	–	–
	nBW2_new	–	–
Second-life	dBW1_SL	daily	one-time experiment
	dBW2_SL	daily	–

* The module name is defined by the backwash frequency (d: daily, w: weekly, 2w: every two weeks and n: never backwash), the abbreviation BW for backwash, the number of the replicate and the module type (new and old).

2.6. Statistical analysis

The average values and standard deviations of the stable flux and biopolymer removal were calculated based on visual observation and selection of the stabilized period. Values were compared using Wilcoxon test, given that the data were independent and not normally distributed (see section 4 in supplementary data). Outliers were not considered in the calculation, using the procedure described in Stoffel et al. (2022). Specifically, the value below Q1–1.5*IQR and above Q3+1.5*IQR were not considered for calculation. Q1 and Q3 correspond to the 25th quantile and 75th quantile, respectively. IQR is the interquantile range, i.e., the difference between Q3 and Q1.

2.7. Costs calculations

We evaluated the cost of membranes and the OPEX for several energy costs to generate 1000 m^3/h over a 25-year period, costs in order to compare them and assess the economic viability of GDM filtration compared to conventional UF. All calculations were made with a membrane surface of 80 m^2, as it is the membrane surface of dizzer XL 0.9 MB 80 WT modules equipped with the membrane tested in the present study. The number of modules for each scenario was calculated using Eq. (1):

$$N = R_m \times \frac{F_{plant}}{Q_{membrane} \times A} \quad (1)$$

With N the number of modules, R_m the ratio to compensate the productivity loss due to maintenances, F_{plant} the plant productivity (m^3/h), $Q_{membrane}$ the stable flux (m^3/m^2/h) and A the module membrane surface area (m^2). R_m values are listed in Table S1 in supplementary data.

The costs of membranes over a 25 years period was calculated using the following formula:

$$Membrane_{costs} = N_{modules} \times \frac{P_{module} \times T_{costs}}{T_{module} \times V_{plant}} \times 100 \quad (2)$$

With $Membrane_{costs}$ the costs of membrane investments during period over which the costs are calculated (cents€/m^3), P_{module} the pricing per module (€), T_{costs} the period over which the costs are calculated (year), T_{module} the module lifetime (year) and V_{plant} the volume of treated water during the period over which the costs are calculated (m^3).

To calculate the membrane costs, we used a price of 2000 € based on pricing that we found on the website of a membrane supplier (Pureaqua, INC®) given that membrane pricing of inge DuPont is submitted to confidentiality. The membrane costs scenarios using second-life modules were estimated as 5.5 times lower than new modules; this price includes the cleaning and quality check before reuse.

Then we calculated the operating costs using the following formula:

$$OPEX_{UF} = OPEX_{energyUF} + OPEX_{chemicalUF} \quad (3)$$

With $OPEX_{UF}$ the overall operational costs corresponding to energy requirements for filtration and backwash, and chemical cleanings in conventional UF (cents€/m^3), $OPEX_{energyUF}$ the operational costs corresponding to energy requirements for the operation (cents€/m^3), $OPEX_{chemicalUF}$ the operational costs corresponding to chemical requirements for the operation (cents€/m^3). For GDM filtration, we set $OPEX_{chemical}$ to zero. For conventional UF, we assumed that the conventional UF OPEX would correspond to 20% of the $OPEX_{energy}$, based on inge DuPont expertise. Consequently, OPEX was equal to 1.2 $OPEX_{energy}$.

For energy requirements, we proceeded to calculations at different energy costs, given that Europe is facing unprecedent energy costs increase, which might continue in the future. As a consequence, we considered three energetic scenarios, i.e. different costs per MWh: (1) 50 €/MWh corresponding to the energy cost in 2020, (2) 500 €/MWh, Switzerland energy cost in August 2022 and (3) 1000 €/MWh,

Switzerland hypothetical energy cost as projection in the future based on the trend observed at in the second half of 2022 (Statista, 2022).

$$OPEX_{energyUF} = R_m \times \frac{E_{UF}}{1000} \times P_{energy} \times 100 \quad (4)$$

With E_{UF} the energy requirements of conventional UF per cubic meter (kWh/m^3) and P_{energy} the energy price (€/MWh). We used an energetic consumption of 0.02 kWh/m^3 based on inge DuPont experience.

For the OPEX of GDM, the costs would be associated to the pump used to transfer a portion of the permeate to the backwash tank and depend on the water head and the flux using Eq. (5):

$$OPEX_{energy\_GDM} = \frac{Q_{backwas\_tank} \times \Delta P \times T_{operation} \times P_{energy}}{\eta \times V_{plant} \times 10^4} \quad (5)$$

With $OPEX_{energy\_GDM}$ the operational costs corresponding to energy requirements to fill the backwash tank in GDM filtration (cents€/m^3), $Q_{backwash\_tank}$ the flux of permeate that is pumped to the backwash tank (m^3/s), ΔP the water head targeted by the pump (Pa), $T_{operation}$ the number of operation hours during the period over which the costs are calculated (h) and η the pump efficiency. For $Q_{backwash\_tank}$ we used 3% of the plant production, as we determined that the volume used for backwash corresponded to 3% of the daily production and η was fixed to 0.71.

Using the above listed formulas and data from Tables S1 and S2 in supplementary data (section 5), we compared the scenarios listed in Table 4.

We set the lifetime of conventional UF modules to 8 years based on inge DuPont expertise, reflecting typical replacement rate in drinking water treatment plants. This lifetime can be explained by membrane aging leading to permeability reduction and/or integrity loss due to pressure rating and chemical stress (Zondervan and Roffel, 2008; Verrecht et al., 2010). For the GDM modules, there are no references on membrane lifetime since that this approach has only been used in practice for a decade. In the present study, we hypothesized that the GDM modules would have a longer lifetime than conventional UF modules due to the absence of chemical cleaning and pressure rating (Pronk et al., 2019). In particular, we set membrane lifetimes of 15 and 25 years to discuss the impact of this parameter on the membrane investment costs. In addition to evaluate the lifetime effect on the membrane investment costs, we proceeded to calculations with different stable flux values to evaluate the effect of feed water quality on the membrane investment costs, as the stable flux is dependent on the dissolved organic composition of the feed water (Pronk et al., 2019). We used the 10 L/m^2/h as a reference value for values obtained in the present study with river water, i.e., daily backwash new and second-life membranes. The other flux values used for calculations are in line with what might be possible using different feed waters (Peter-Varbanets et al., 2010).

All raw data collected for the study are available at https://doi.org/10.25678/000830.

Table 4
Description of the scenarios used for the calculations.

Process	Module type	Module lifetime (year)	Flux (L/m^2/h)
UF	New	8	70
GDM	New	15	10, 7.5, 5.0 and 2.5
GDM	Second-life	15	10, 7.5, 5.0 and 2.5
GDM	New	25	10, 7.5, 5.0 and 2.5
GDM	Second-life	25	10, 7.5, 5.0 and 2.5

3. Results and discussion

3.1. Intermittent gravity-driven backwash as a strategy to use inside-out hollow fiber membranes for GDM filtration

3.1.1. Effect of gravity-driven backwash on the flux and productivity

Gravity-driven backwash is a relevant strategy to compensate the continuous flux drop observed during the operation without backwash, and leading to a low stable flux, as observed in Fig. 2A. In the present study, the flux of never backwashed modules dropped to 1.4 ± 0.6 L/m^2/h at day 142, which is comparable to the flux measured by Stoffel et al. (2022) after 125 days of operation (between 0 and 2 L/m^2/h). The higher the backwash frequency, the more stable and the higher the flux. Specifically, application of a daily gravity-driven backwash helped stabilizing the flux at 10.6 ± 2.0 L/m^2/h after 20 days of operation at a TMP of 150 mbar (Fig. 2D). This stable flux value was within the same range as what was observed when flat sheet membranes, i.e., low compactness, were utilized in dead-end to filter the same type of water as in the present investigation (Peter-Varbanets et al., 2010; Desmond et al., 2018a). When the backwash was applied every two weeks or weekly, the flux was improved but then dropped at a similar rate for both backwash frequencies (p-value = 0.5), equal to 0.63 ± 0.30 L/m^2/h/d and 0.58 ± 0.32 L/m^2/h/d, respectively (Fig. 2B and 2C). Our results demonstrate that the use of compact membrane geometries such as hollow-fibers for GDM filtration is possible only if a backwash is applied at a frequency that balances the continuous flux drop triggered by high module compactness.

The implementation of a membrane module with compact geometry comes with additional costs related to the daily backwash, compared to GDM filtration without maintenance (Oka et al., 2017). However, since we showed that the daily backwash could be gravity-driven, backwash costs could be minimized; the energy to pump the permeate to the backwash tank is height time lower than the energy required for a pressurized backwash. The consumption of permeate for backwash is another crucial factor to consider in order to evaluate the approach discussed in our study, because it lowers plant productivity. GDM filtration gravity-driven backwash would require 3% of the daily production, against 7% and 4% with a pressurized backwash of GDM filtration and conventional UF based on calculations with values from Table S1, respectively. Therefore, the permeate requirements for gravity-driven backwash GDM filtration are on level with those for conventional UF. These requirements are even lower than requirements found in literature: conventional UF pressurized backwash can consume up to 10% of permeate, given that modules are backwashed every 30 min to 4 h for 1 to 5 min (Brügger et al., 2001; Chang et al., 2017).

3.1.2. Link between flux recovery and TSS removal from the lumen through gravity-driven backwash

In parallel to flux measurements, we systematically evaluated the link between flux recovery after each backwash and the amount of TSS collected in the backwash water, to understand the flux dynamic observed for the different backwash frequencies (Fig. 3).

The flux recovery triggered by the backwash was linked to the removal of TSS from the HF lumen (Fig. 3): the higher the amount of TSS removed, the higher the flux recovery (R^2 of 0.646, p-value = 1×10^{-7}). For weekly and every two weeks backwash conditions, the removal of TSS was around 6 times higher than for the daily backwash. However, removing less TSS at once by increasing backwash frequency was more strategic to maintain a stable flux. These results highlight that the accumulation of TSS in the lumen triggers the continuous flux drop observed with compact membrane geometries. In our study, the accumulation of TSS was likely linked to biofilm growth, given the low turbidity in the feed water and the small size of particles compared to the lumen (Table 2). For low backwash frequencies, the fiber lumen was progressively obstructed as the biofilm grew, reducing water flow in the lumen and causing flux drop.

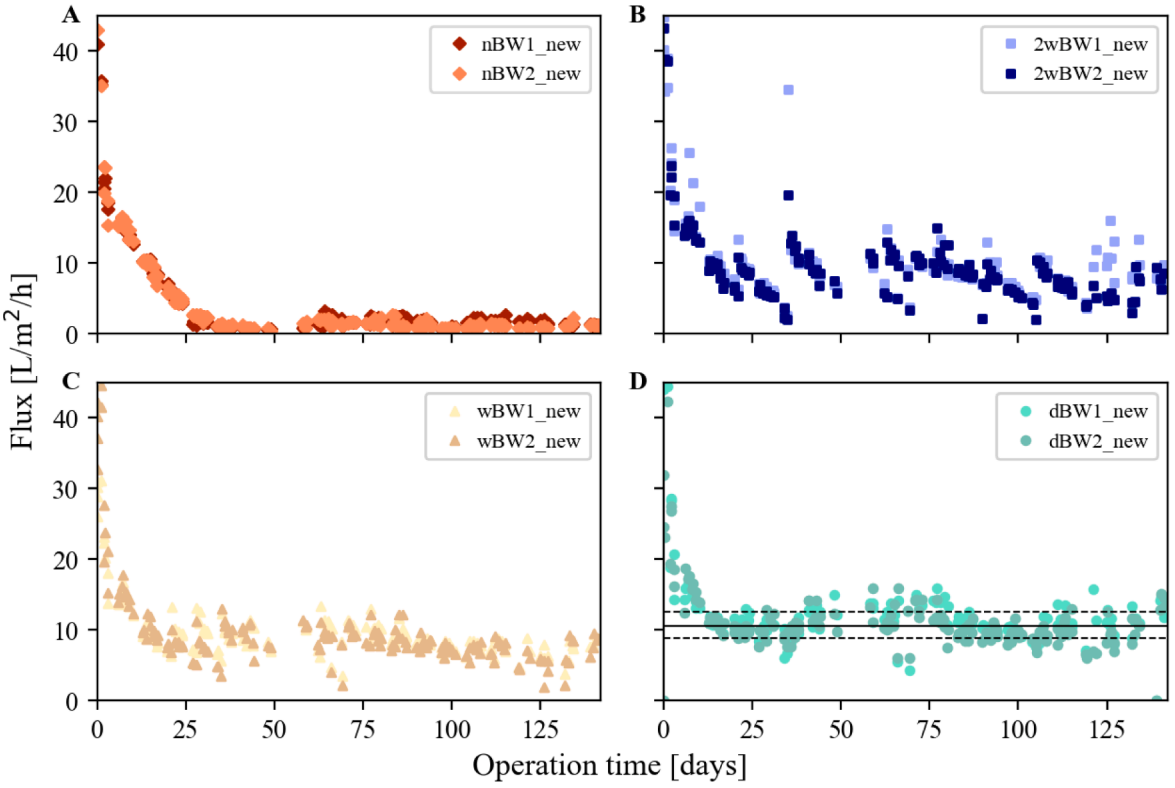

Fig. 2. Permeate flux over operational time of modules equipped with new membranes (A) never backwashed, (B) backwashed every two weeks, (C) weekly backwashed and (D) daily backwashed. The numbers 1 and 2 correspond to duplicates. The black horizontal lines in B, C and D panel correspond to the mean flux values calculated between day 20 and day 142. The upper and lower horizontal dotted black lines in D panel correspond to Q3+1.5*IQR and Q1–1.5*IQR of the flux values between day 20 and day 142, respectively. Backwash flux values are available in Fig. S4 in supplementary data.

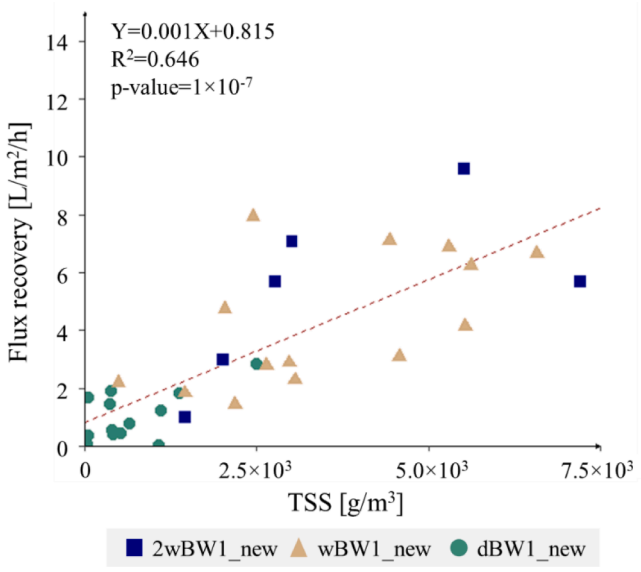

Fig. 3. Permeate flux recovery as a function of the amount of TSS collected during the backwash of modules equipped with new membranes backwashed at different frequency: every two weeks (2wBW1_new), weekly (wBW1_new) and daily (dBW1_new). Raw flux recovery data are listed in Table S3 in supplementary data.

We expect that organics causing irreversible membrane fouling, i.e., that cannot be eliminated by the backwash (e.g., humic substances), played a limited role on the flux drop compared to the biofilm. Previous studies reported that 80 to 90% of the resistance in GDM systems equipped with flat sheet membranes is due to biofilm and depends on biofilm physico-chemical properties (Desmond et al., 2018c; Jafari et al., 2018). In the context of compact membranes, the proportion of the biofilm resistance could even be higher due to lumen blockage. The limited role of organics in flux drop is also supported by the fact that the mean hydraulic resistances at the beginning and end of the period of stable flux (first and last 20d) of the daily backwashed modules are similar: $2.9 \times 10^{12} \pm 0.5 \times 10^{12}$ 1/m and $2.8 \times 10^{12} \pm 0.6 \times 10^{12}$ 1/m, respectively (p-value=0.07). Significant irreversible fouling would have gradually increased the hydraulic resistance, as observed in conventional UF (Gao et al., 2011; Zheng et al., 2014).

Similar hydraulic resistance at the start and end of the steady flux period further demonstrates that the daily backwash has no detrimental effects on the biofilm over the 142 days of the study; the flux was improved by the gravity-driven backwash without having triggered biofilm acclimation, which would have gradually decreased the flux. Wu et al. (2019) observed that membrane resistance increased from $\sim 3.5 \times 10^{12}$ 1/m to $\sim 5 \times 10^{12}$ 1/m between modules operated without backwash and modules operated with a 2 min backwash applied at different intervals, respectively. The increase of resistance could be explained by biofilm adaptation to the shear stress, which enhances the secretion of extracellular polymeric substances and promotes self-reorganization, (Derlon et al., 2016; de Vries et al., 2021). For instance, Derlon et al. (2022) showed that the biofilm became more cohesive and elastic as a result of surface shear stress brought on by cross flow maintenance. The absence of hydraulic resistance increase in our study might be due to the fact that hydraulic resistance of compact modules might be more dependent on fiber blockage than on the characteristics of the biofilm. To better understand the cause of the continuous flux drop, more studies of biofilm characteristics using methods like OCT would be particularly interesting (Desmond et al., 2018a; 2018b, 2018c; Fortunato et al., 2020). As the biofilm develops in the

fibers' lumen, this would necessitate the sacrifice of the modules.

In conclusion, we successfully demonstrated that maintaining high stable flux values (> 10 L/m^2/h) with compact membrane geometry, i.e., inside-out HF with an inner diameter of 0.9 mm, is possible with a daily gravity-driven backwash implemented to control biofilm growth in the fiber's lumen.

3.2. Potential of second-life modules as an alternative for new modules in GDM filtration systems

3.2.1. Comparison of second-life and new membrane properties before GDM filtration experiments

To compensate the cost increase linked to lower flux compared to conventional UF, we assessed if modules with second-life membranes had similar filtration performance than modules with new membranes. Beforehand, we compared their permeability and noticed that the permeability of second-life modules was 19% lower in average than the permeability of new modules (Table 1). We then proceeded to SEM imaging of the inside and outside of new and second-life membranes (Fig. 4).

The SEM images revealed that there were distinct surface properties between new and second-life membranes, despite identical membrane elaboration process. The inside surface of the new membrane appeared smoother than that of the second-life membrane, except for some visible gray spots in Fig. 4A. However, these spots were likely artifacts caused by the sample preparation process. On the other hand, the inside surface of the second-life membrane displayed more visible pores, which may be due to frequent chemical cleaning that enlarges the pores, as reported in previous studies (Regula et al., 2014; Li et al., 2021). Changes of surface properties were also visible on the outside of the membrane. The outside surface of the second-life membrane was found to be rougher than the outside of the new membrane, with a higher pore density like for the inside. This could be also be due to aging of the membrane linked to chemical cleaning. In addition, deposits and blocked particles were observed in the outside pores of the second-life membrane (see Fig. S5 in supplementary data), which could explain the differences in permeability between the new and second-life membranes. The changes observed between new and second-life membranes are consistent with literature, where membrane properties change when soaking them in NaOCl (Robinson and Bérubé, 2021). Finally, these findings confirm that new and second-life membranes have noticeable surface physical differences, which could affect the GDM filtration performance in terms of flux and biopolymer removal.

3.2.2. Flux of second-life modules operated in GDM filtration mode

We monitored the permeate flux over several weeks of modules equipped with second-life 0.9 mm inside-out 7-capillaries HF operated in GDM filtration with a daily gravity-driven backwash (Fig. 5).

After 20 days of operation, we observed that the flux of modules with second-life membranes stabilized at 9.2 ± 1.4 L/m^2/h until day 142, i.e., 13% lower than the flux value measured for modules with new membranes (Wilcoxon test p-value = 2×10^{-16}) (Fig. 2D). This value remains close to the value obtained with modules with new membranes and is comparable to the flux of other GDM systems run with new membranes and river water as feed (Peter-Varbanets et al., 2010). In addition, second-life membranes allowed us to achieve a stable flux value that was

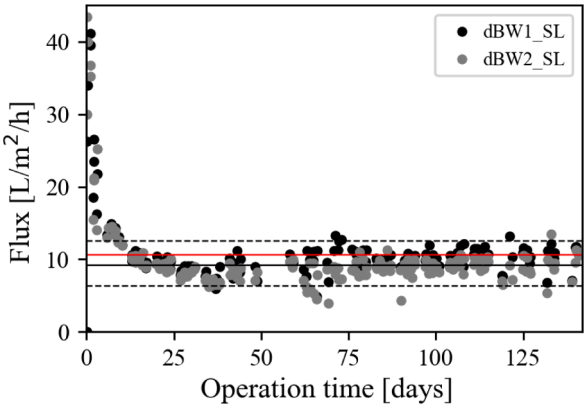

Fig. 5. Permeate flux over operational time of modules equipped with second-life membranes daily backwashed. The upper and lower horizontal dotted black lines correspond to Q3+1.5*IQR and the Q1–1.5*IQR values of the flux between day 20 and day 142, respectively. The red line is the mean flux value calculated for dBW_new modules.

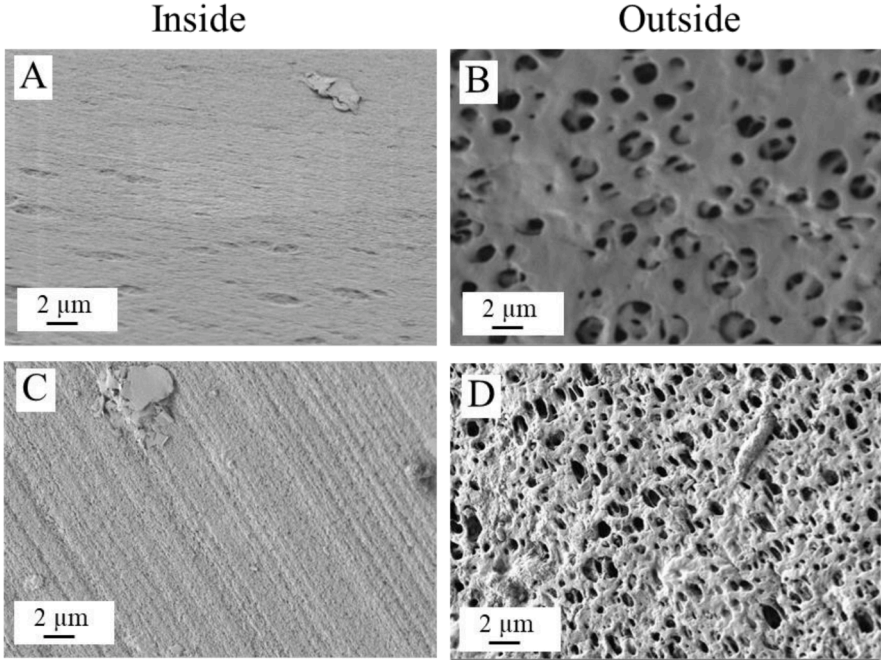

Fig. 4. SEM images of (A) inside of new membrane, (B) outside of new membrane, (C) inside of second-life membranes and (D) outside of second-life membranes.

significantly larger than the flux that was measured by García-Pacheco et al. (2021) with reconditioned RO modules. A lower permeability for second-life modules than for new modules at the start of the experiment could account for this minor stable flux difference over long term between new and second-life modules (Table 1). This flux difference was, however, minimal and could quickly be reduced over time with a decrease of new membranes permeability during operation. Regula et al. (2013) studied the aging of hollow fiber membranes in pure water with and without sodium bisulfite. The authors showed no decrease of permeability after 30 days of aging, while it was reduced by 26% after 180 days of operation, irrespective the presence of biocide.

As observed for modules with new membranes, the hydraulic resistance measured for modules with second-life membranes daily backwashed was similar in the first and last 20 days operation. It was equal to $3.2 \times 10^{12} \pm 0.6 \times 10^{11}$ 1/m and $3.0 \times 10^{12} \pm 0.5 \times 10^{11}$, respectively (Wilcoxon test p-value=7.3×10^{-7}). It demonstrates that daily gravity backwash is effective at improving the flux of modules with second-life membranes without having an adverse long-term effect on resistance, as observed for modules equipped with new membranes.

Finally, the permeate consumption was similar to GDM filtration with new modules, representing only 2% of the daily production when considering an average backwash flux of 74 L/m^2/h, contrary to what was observed by Cogan et al. (2022). The authors reported that membrane aging induces higher backwash frequency and duration. Last but not least, comparable to GDM filtration with new membranes, we did not notice biofilm adaptation to the backwash as indicated by the similar hydraulic resistance at the beginning/end of the period of stable flux. In conclusion, modules with second-life modules perform as well as modules with new membranes in terms of filtration. The initial membrane properties have a limited effect on the flux, given that most of the resistance is due to the biofilm, independently of the type of membranes (Pronk et al. (2019).

3.3. Impact of the gravity-driven backwash frequency and use of second-life membranes on the biopolymer removal

3.3.1. Long-term biopolymer removal trends

Throughout the entire experiment, we monitored biopolymer removal over time for the modules with new membranes backwashed at different frequencies and for the modules with second-life modules exposed to daily backwash conditions (Fig. 6).

The first key result is that the initial removal of the modules equipped with new membranes and with second-life membranes equal to 21% (dBW1_new) and 11% (dBW1_SL), respectively. This means that membrane aging impacted the membrane retention of biopolymers. Similar result was observed for aged PES membranes: expose to chlorine PES membranes used in the milk industry has been reported to lead to milk protein leakage (Regula et al., 2014). This difference in retention performance could be explained by the increased pore density observed by SEM and decreased retention due to pore widening (Li et al., 2021). Then, all modules showed an increase in biopolymer removal with time, until reaching a plateau after 20 days of operation. This trend is typical from GDM filtration systems and is explained by the progressive establishment of the biofilm at the membrane surface until the biofilm reaches equilibrium state, corresponding to a stable biopolymer removal (Stoffel et al., 2022). When the plateau was reached, we observed two points corresponding to a biopolymer removal of 50.5% and 35.5% for the never backwashed new module and daily backwashed second-life module, respectively. We, however, ruled these values outliers as they were lower than the Q1–1.5*IQR calculated with all removal values of the plateau period (Fig. 6). Without the outliers, the biopolymer removal average was statistically identical for all modules, irrespective the backwash frequency and the module type (Table S5 in supplementation data). The mean biopolymer removal of all modules was equal to 81.8 ± 8.6%, which is similar to the removal observed for GDM systems equipped with flat sheet membranes never backwashed (Chomiak et al., 2015; Pronk et al., 2019). It means that even if biofilm is removed from the lumen during the backwash, as we observed through TSS removal, the biopolymer removal remained at high level. Another important result is that the biopolymer removal trend and values for modules equipped with both new and second-life membranes was similar, despite different initial removal values. This confirms that the presence of biofilm is the primary factor driving biopolymer removal, even if membrane aging results in lower initial removal.

3.3.2. Short-term effect of increased TSS removal by gravity-driven backwash on the biopolymer elimination

The backwash may have a negative effect on biopolymer removal on the short term since it could destabilize the biofilm, as observed by Shao et al. (2018). We noticed that increasing the amount of biofilm (TSS) removed from the lumen through successive backwashes at higher TMP had a slight impact on the short-term removal of biopolymers (Fig. 7). We found a significant linear relationship between the biopolymer removal and the amount of TSS removed by the backwash, which increased with the backwash TMP (p-value = 2×10^{-4}, $R^2 = 0.764$).

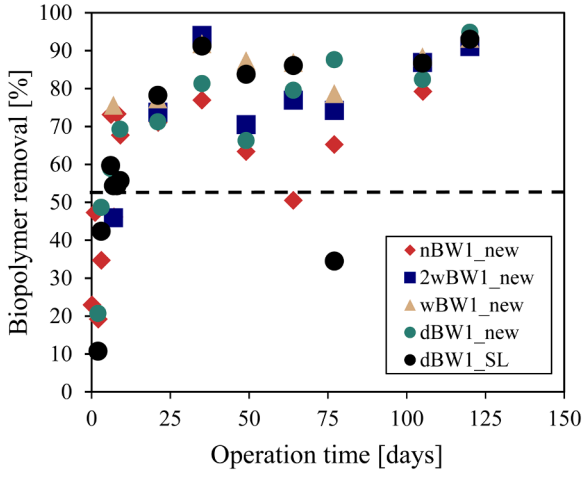

Fig. 6. Biopolymer removal efficiency over operational time. The black dotted line corresponds to the Q1–1.5*IQR calculated on values collected between day 20 and day 142. The Q3–1.5*IQR is not displayed in this plot given that it is equal to 107.7% and no values could be measured above this limit.

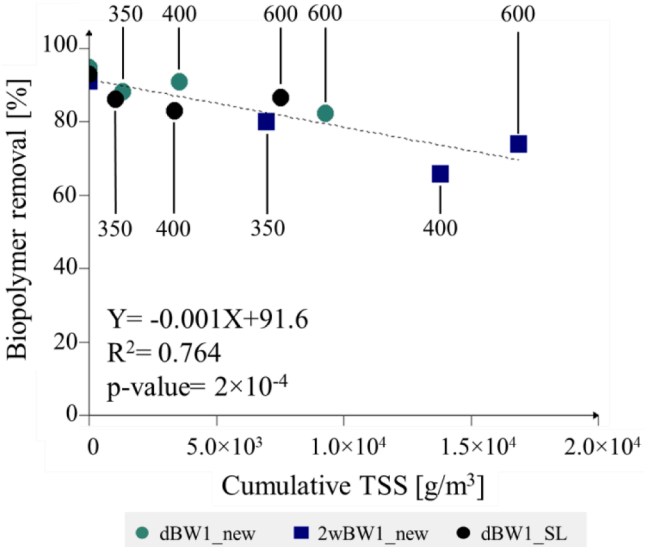

Fig. 7. Biopolymer removal as a function of the cumulative TSS removal. The labels correspond to TMP applied for the considered backwash (mbar).

Consequently, the higher the TSS removed the lower the biopolymer removal. In addition, Fig. 7 shows three key results: (1) the daily gravity-driven backwash (350 mbar) had no short term negative consequences on the biopolymer removal, (2) backwash at higher pressure only slightly decreased the biopolymer removal, but it remained above 67%, which is 47% to 57% higher than the initial removal obtained for modules with new and second-life membranes, respectively, and (3) the performance of new membrane modules and second-life modules were similar, as observed for the long-term biopolymer removal and for the flux. These results mean that in practice it would be possible to use modules with second-life membranes and increase the backwash TMP without negatively affecting the permeate quality.

Therefore, a significant conclusion of our study is that GDM filtration could be carried out with second-life modules without affecting the filtration performance due to high stable flux and biopolymer removal values, which were likewise found for GDM filtration with new modules.

3.4. GDM filtration scenarios economically viable compared to conventional UF

Our experimental results demonstrated that modules with second-life membranes have comparable performance than modules with new membranes in terms of both stable flux and biopolymer removal. The next step was to identify under which scenario GDM filtration could represent a relevant alternative to conventional UF for centralized facilities, rather than a niche application for decentralized facilities only. Pronk et al. (2019) indeed stated that GDM filtration is confined to decentralized systems given the high membrane investment costs compared to conventional UF. In a recent study calculating the membrane investment costs and operating costs of a GDM filtration home system using refurbished RO modules, the authors estimated that the costs of GDM filtration and UF systems could be equivalent (García-Pacheco et al., 2021). However, these data were provided for decentralized facilities, and the stable flux values are noticeably low and may have been overstated due the extremely short filtration test duration as previously mentioned.

Fig. 8 compares the membrane costs for membrane and the OPEX per m^3 of conventional UF, GDM with new membranes and GDM filtration with second-life membranes for different stable flux values and membrane lifetime. In this figure, we also compared the impact of different energy pricing on the OPEX.

The membrane costs of UF was equal to 0.54 cents€/m^3 when considering a membrane lifetime of 8 years and a stable flux of 70 L/m^2/h. To be competitive in terms of membrane investment costs, GDM filtration costs should therefore be lower than 0.54 cents€/m^3. When considering a GDM filtration stable flux of 10 L/m^2/h as observed in our study, the membrane costs of GDM filtration with second-life modules was 14 and 57% lower than for conventional UF when considering a membrane lifetime of 15 and 25 years, respectively. Other scenarios had lower membrane investments costs, such as GDM filtration with second-

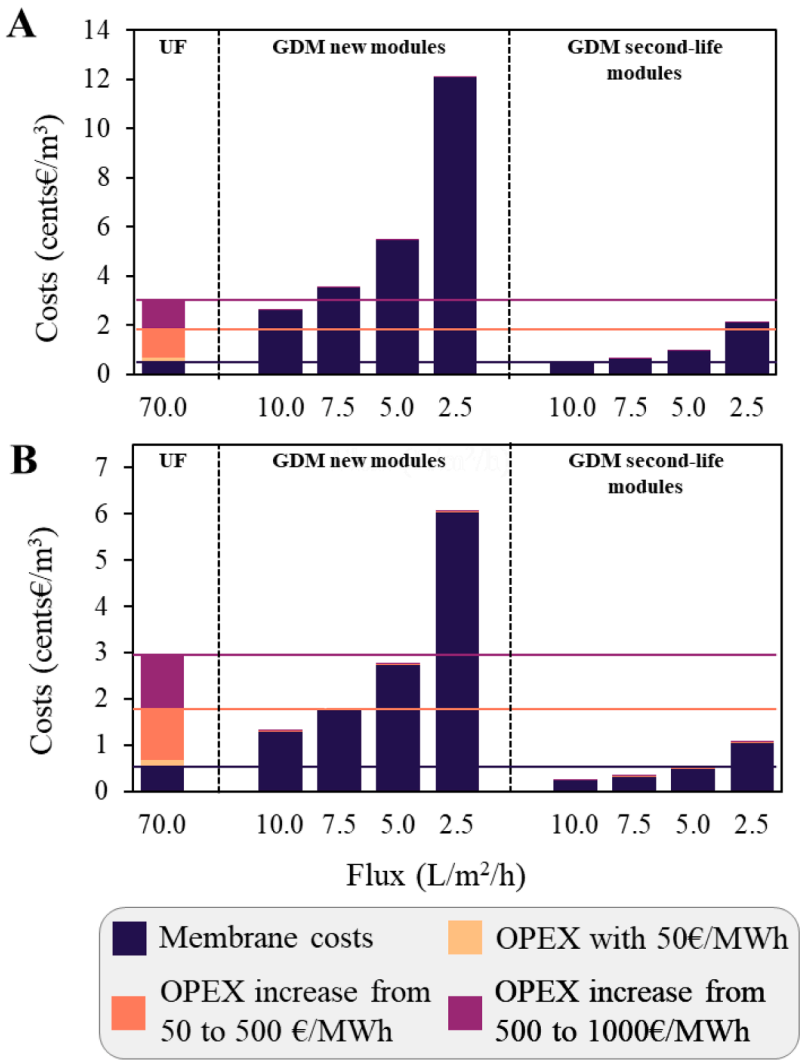

Fig. 8. Comparison of the membrane costs and OPEX of conventional UF and GDM filtration with modules equipped with new and second-life membrane for a GDM membrane lifetime of (A) 15 years and (B) 25 years. The horizontal lines correspond to conventional UF membrane costs (dark blue), conventional UF membrane costs + OPEX for an energy pricing of 500 €/MWh (orange) and conventional UF membrane costs + OPEX for an energy pricing of 1000 €/MWh (purple). No line was added for conventional UF membrane costs + OPEX for an energy pricing of 50 €/MWh given that the OPEX at an energy cost of 50 €/MWh was 10 times lower than membrane costs, i.e., not visible at the scales chosen for the plots.

life modules at a stable flux of 7.5 and 5.0 L/m^2/h and a membrane lifetime of 25 years. These findings show that, there are cases where GDM filtration could be less expensive than conventional UF, despite higher surface membrane requirements for GDM filtration. The significant difference in membrane prices between GDM filtration using second-life modules and conventional UF is explained by reduced module costs (5.5 times lower) and a lower replacement rate for the GDM membranes. Over a period of 25 years, conventional UF modules were replaced three times, versus twice and once for GDM membranes replaced after 25 and 15 years of operation. However, we confirmed that, regardless of the lifespan of GDM membranes, membrane investment costs of new modules remained greater than with conventional UF, as reported by Pronk et al. (2019). Nevertheless, extending GDM membrane lifetime of new modules from 15 to 25 years made GDM filtration more appealing by lowering membrane costs across all scenarios. For instance, the membrane costs of GDM filtration with new modules having a stable flux of 10 L/m^2/h were reduced from 2.59 to 1.29 cents€/m^3 when considering a lifetime extension from 15 to 25 years. Conducting further research on how to accurately estimate the lifespan of modules used in GDM filtration (new and second-life) could assist in determining the actual cost benefits as compared to conventional UF. The stable flux value also played a significant role in the membrane investment costs, given that the lower the stable flux, the higher the required number of modules. For instance, at a stable flux of 2.5 L/m^2/h and a lifetime of 15 years, membrane investment costs of GDM filtration with new and second-life modules were equal to 12 and 2 cents€/m^3, respectively. These costs are considerably higher than membrane investment costs of conventional UF.

To evaluate the economic viability of GDM filtration scenarios, we then considered the impact of OPEX changes due to energy pricing evolution. At an energy pricing of 50 €/MWh (price in 2020), we could observe that the determinant factor for the total costs was membrane investment costs for both conventional UF and GDM filtration, as the OPEX was equal to 0.13 cents€/m^3 for conventional UF and 1.6×10^{-3} cents€/m^3 for GDM filtration (costs not visible with the scale chosen for Fig. 8). The OPEX only accounted for 19% in the case of conventional UF, while for GDM filtration it was less than 0.3% depending on the scenario. However, in a situation where energy pricing skyrocketed because of lack of energy autonomy in Europe (500 €/MWh - August 2022), the OPEX accounted for 70% of the total costs of conventional UF, and therefore became a determinant cost factor. GDM filtration, on the other hand, was unaffected by the rise in energy prices, despite the use of a pump to increase the permeate water head for the gravity-driven backwash. In the event that the energy situation worsens in the future and prices reach values as high as 1000 €/MWh, other new GDM filtration scenarios would be advantageous compared to conventional UF: GDM filtration operating at stable flux of 7.5 and 5.0 L/m^2/h. GDM filtration using new membrane modules with a stable flux of 10.0 L/m^2/h would even be less expensive than conventional UF. Such scenarios are relevant to consider, as a projected energy cost of 1000 €/MWh may become a reality in the future, given the other factors that are currently threatening non-carbonated energy self-sufficiency, such as droughts that decrease the electricity generation of hydropower plants (Thaler and Hofmann, 2022; Turner et al., 2022).

Our results showed that it was crucial to consider the OPEX to evaluate economic viability of GDM filtration compared to conventional UF. Energy price increases that were seen in Europe over the past two years had no influence on overall GDM filtration costs, but had a negative impact on conventional UF. This observation demonstrates that (1) GDM filtration is a process that can enable more resilient drinking water production in centralized facilities in the event of an energy crisis and even in the event of an electricity outage and (2) GDM filtration is more economically viable than conventional UF the higher the energy costs. Between August 2020 and August 2022, the factor 10 energy cost increase boosted the membrane cost-to-OPEX ratio of conventional UF for from 1.2 to 3.3. As a result, the majority of GDM filtration scenarios with second-life modules considered for our analysis were less expensive than conventional UF after the energy pricing skyrocketed. For a membrane lifetime of 25 years, even the scenario with a stable flux of 2.5 L/m^2/h was economically viable, which could correspond to the flux obtained with a feed water with high organic contents. This means that GDM filtration could be used to produce drinking water from sources of various quality levels since the stable flux value is greatly influenced by the TOC content of the input water (Peter-Varbanets et al., 2010). Furthermore, if energy costs continue to rise in the future, there could be a growing economic incentive to use GDM filtration. The OPEX could gradually become the main expense of conventional UF, making GDM filtration economically viable even with new membrane modules, as we started to observe for energy cost of 500 €/MWh and higher and membrane lifetime of 25 years.

In conclusion, our study permitted to give a first estimation of the economic interest of using GDM filtration as an alternative to conventional UF in centralized drinking water treatment facilities in multiple scenarios. These scenarios depend on the stable flux, membrane lifetime and energy costs and GDM filtration; the decision of where to implement GDM filtration should be made on a case-by-case basis, considering these factors. For a better estimation of the optimal implementation of GDM filtration in centralized systems, it would be strategic to develop a business model considering other factors including the number of modules that would be disposed by drinking water treatment plants. Currently, data on UF waste production are scarce in literature, but there are several detailed reports for RO modules (García-Pacheco et al., 2015; Lawler et al., 2015; Senán-Salinas et al., 2019). According to Landaburu-Aguirre et al. (2016), Spain annually discards more than 1000 tons of modules in landfills. We could expect that the amount of decommissioned UF modules is in the same order of magnitude, and would tendentially increase in the future due to increased water contamination and more stringent regulations (Al Aani et al., 2020). The business model should also consider factors such as recycling and transport procedures, and their impact on second-life module costs, the water source considered for treatment, the benefits of recycling the modules based on life cycle assessment, need for resilience, as well as the space requirements and space constraints.

Conclusions

- We demonstrated that GDM filtration in centralized facilities is technically and economically feasible in a variety of scenarios that depend on stable flux, membrane lifetime and energy costs. In these scenarios, replace conventional UF by GDM filtration would increase the resilience of the drinking water supply at centralized facilities, given that GDM filtration has a reduced reliance on energy, chemicals, and membrane modules.
- We demonstrated that it is technically possible to obtain stable fluxes around 10 L/m^2/h with compact modules operated in GDM filtration mode, i.e., modules equipped with inside-out hollow fibers having an inner diameter of 0.9 mm, with a daily gravity-driven backwash. In terms of permeate quality, the daily backwash had no negative effect on the biopolymer removal compared to modules that were maintained with relaxation and forward flush.
- Modules with second-life membranes had stable flux in a comparable range than modules with new membranes and performed similarly in terms of biopolymer removal, even if initial permeability and biopolymer removal was lower. This shows that using refurbished UF modules for GDM filtration is a feasible and strategic.
- GDM filtration membrane investment costs were significantly lowered by using modules with second-life membranes, even if modules requirements were minimum 2.3 times higher than for conventional UF. With this strategy, we identified a scenario in which GDM filtration was less expensive than conventional UF at low energy pricing for the first time: with second-life modules having a stable flux of 10.0 L/m^2/h and a membrane lifetime of 25 years, GDM

filtration's membrane investment costs were 14% lower than those of conventional UF.

- When considering fluctuation of energy costs to evaluate the economic viability of GDM filtration, we highlighted two key results: (1) GDM filtration overall costs were not affected by changes in energy pricing, contrary to conventional UF, and (2) energy costs increase made several scenarios for the deployment of GDM filtration in centralized facilities economically viable, including scenarios with new membrane modules and scenarios with stable flux values as low as 5.0 L/m^2/h.

Declaration of Competing Interest

The authors declare that they have no known competing financial interests or personal relationships that could have appeared to influence the work reported in this paper.

Data availability

The data will be available on Eawag depositary. The doi of the data package is provided in the manuscript.

Acknowledgments

The support of discretionary funding from Eawag is gratefully acknowledged.

Supplementary materials

Supplementary material associated with this article can be found, in the online version, at doi:10.1016/j.wroa.2023.100178.

References

Akhondi, E., Wu, B., Sun, S., Marxer, B., Lim, W., Gu, J., Liu, L., Burkhardt, M., McDougald, D., Pronk, W., Fane, A.G., 2015. Gravity-driven membrane filtration as pretreatment for seawater reverse osmosis: Linking biofouling layer morphology with flux stabilization. Water Res. 70, 158–173. https://doi.org/10.1016/j.watres.2014.12.001.

APHA, 2005. Standard Methods for the Examination of Water and Wastewater, 19th Ed. American Water Works Association and the Water Environment Federation, Washington, D.C.

Brügger, A., Voßenkaul, K., Melin, T., Rautenbach, R., Golloing, B., Jacobs, U., Ohlenforst, P., 2001. Reuse of filter backwash water by implementing ultrafiltration technology. Water Supply 1, 207–214. https://doi.org/10.2166/ws.2001.0116.

Chang, H., Liang, H., Qu, F., Liu, B., Yu, H., Du, X., Li, G., Snyder, S.A., 2017. Hydraulic backwashing for low-pressure membranes in drinking water treatment: a review. J. Memb. Sci. 540, 362–380. https://doi.org/10.1016/j.memsci.2017.06.077.

Chomiak, A., Traber, J., Morgenroth, E., Derlon, N., 2015. Biofilm increases permeate quality by organic carbon degradation in low pressure ultrafiltration. Water Res. 85, 512–520. https://doi.org/10.1016/j.watres.2015.08.009.

Cogan, N.G., Ozturk, D., Ishida, K., Safarik, J., Chellam, S., 2022. Membrane aging effects on water recovery during full-scale potable reuse: mathematical optimization of backwashing frequency for constant-flux microfiltration. Sep. Purif. Technol. 286, 120294 https://doi.org/10.1016/j.seppur.2021.120294.

de Vries, H.J., Kleibusch, E., Hermes, G.D.A., van den Brink, P., Plugge, C.M., 2021. Biofouling control: the impact of biofilm dispersal and membrane flushing. Water Res. 198, 117163 https://doi.org/10.1016/j.watres.2021.117163.

Derlon, N., Desmond, P., Rühs, P.A., Morgenroth, E., 2022. Cross flow frequency determines the physical structure and cohesion of membrane biofilms developed during gravity-driven membrane ultrafiltration of river water: implication for hydraulic resistance. J. Memb. Sci. 120079 https://doi.org/10.1016/j.memsci.2021.120079.

Derlon, N., Grütter, A., Brandenberger, F., Sutter, A., Kuhlicke, U., Neu, T.R., Morgenroth, E., 2016. The composition and compression of biofilms developed on ultrafiltration membranes determine hydraulic biofilm resistance. Water Res. 102, 63–72. https://doi.org/10.1016/j.watres.2016.06.019.

Derlon, N., Mimoso, J., Klein, T., Koetzsch, S., Morgenroth, E., 2014. Presence of biofilms on ultrafiltration membrane surfaces increases the quality of permeate produced during ultra-low pressure gravity-driven membrane filtration. Water Res. 60, 164–173. https://doi.org/10.1016/j.watres.2014.04.045. https://www.sciencedirect.com/science/article/abs/pii/S0043135414003303.

Desmond, P., Best, J.P., Morgenroth, E., Derlon, N., 2018a. Linking composition of extracellular polymeric substances (EPS) to the physical structure and hydraulic resistance of membrane biofilms. Water Res. 132, 211–221. https://doi.org/10.1016/j.watres.2017.12.058.

Desmond, P., Böni, L., Fischer, P., Morgenroth, E., Derlon, N., 2018b. Stratification in the physical structure and cohesion of membrane biofilms — Implications for hydraulic resistance. J. Memb. Sci. 564, 897–904. https://doi.org/10.1016/j.memsci.2018.07.088.

Desmond, P., Morgenroth, E., Derlon, N., 2018c. Physical structure determines compression of membrane biofilms during Gravity Driven Membrane (GDM) ultrafiltration. Water Res. 143, 539–549. https://doi.org/10.1016/j.watres.2018.07.008.

Fortunato, L., Ranieri, L., Naddeo, V., Leiknes, T., 2020. Fouling control in a gravity-driven membrane (GDM) bioreactor treating primary wastewater by using relaxation and/or air scouring. J Memb Sci 610, 118261. https://doi.org/10.1016/j.memsci.2020.118261.

Gao, W., Liang, H., Ma, J., Han, M., Chen, Z., Han, Z., Li, G., 2011. Membrane fouling control in ultrafiltration technology for drinking water production: a review. Desalination 272, 1–8. https://doi.org/10.1016/j.desal.2011.01.051.

García-Pacheco, R., Landaburu-Aguirre, J., Molina, S., Rodríguez-Sáez, L., Teli, S.B., García-Calvo, E., 2015. Transformation of end-of-life RO membranes into NF and UF membranes: evaluation of membrane performance. J. Memb. Sci. 495, 305–315. https://doi.org/10.1016/j.memsci.2015.08.025.

García-Pacheco, R., Li, Q., Comas, J., Taylor, R.A., Le-Clech, P., 2021. Novel housing designs for nanofiltration and ultrafiltration gravity-driven recycled membrane-based systems. Sci. Total Environ. 767, 144181 https://doi.org/10.1016/j.scitotenv.2020.144181.

Hawari, A.H., Hafiz, M., Yasir, A.T., Alfahel, R., Altaee, A., 2020. Evaluation of ultrafiltration and multimedia filtration as pretreatmeprocess for forward osmosis.

Huber, S.A., Balz, A., Abert, M., Pronk, W., 2011. Characterisation of aquatic humic and non-humic matter with size-exclusion chromatography – organic carbon detection – organic nitrogen detection (LC-OCD-OND). Water Res. 45, 879–885. https://doi.org/10.1016/j.watres.2010.09.023.

Jacquin, C., Yu, D., Sander, M., Domagala, K.W., Traber, J., Morgenroth, E., Julian, T.R., 2020. Competitive co-adsorption of bacteriophage MS2 and natural organic matter onto multiwalled carbon nanotubes. Water Res. X (9), 100058. https://doi.org/10.1016/j.wroa.2020.100058.

Jafari, M., Desmond, P., van Loosdrecht, M.C.M., Derlon, N., Morgenroth, E., Picioreanu, C., 2018. Effect of biofilm structural deformation on hydraulic resistance during ultrafiltration: a numerical and experimental study. Water Res. 145, 375–387. https://doi.org/10.1016/j.watres.2018.08.036.

Landaburu-Aguirre, J., García-Pacheco, R., Molina, S., Rodríguez-Sáez, L., Rabadán, J., García-Calvo, E., 2016. Fouling prevention, preparing for re-use and membrane recycling. Towards circular economy in RO desalination. Desalination, Fouling and Scaling in Desalination 393, 16–30. doi:10.1016/j.desal.2016.04.002.

Lawler, W., Alvarez-Gaitan, J., Leslie, G., Le-Clech, P., 2015. Comparative life cycle assessment of end-of-life options for reverse osmosis membranes. Desalination 357, 45–54. https://doi.org/10.1016/j.desal.2014.10.013.

Lawler, W., Antony, A., Cran, M., Duke, M., Leslie, G., Le-Clech, P., 2013. Production and characterisation of UF membranes by chemical conversion of used RO membranes. J Memb Sci 447, 203–211. https://doi.org/10.1016/j.memsci.2013.07.015.

Li, K., Su, Q., Li, S., Wen, G., Huang, T., 2021. Aging of PVDF and PES ultrafiltration membranes by sodium hypochlorite: effect of solution pH. Journal of Environmental Sciences 104, 444–455. https://doi.org/10.1016/j.jes.2020.12.020.

Maghsoodi, M., Jacquin, C., Teychené, B., Heran, M., Tarabara, V.V., Lesage, G., Snow, S. D., 2019. Emerging investigator series: photocatalysis for MBR effluent post-treatment: assessing the effects of effluent organic matter characteristics. Environ. Sci.: Water Res. Technol. 5, 482–494. https://doi.org/10.1039/C8EW00734A.

Mišík, M., 2022. The EU needs to improve its external energy security. Energy Policy 165, 112930. https://doi.org/10.1016/j.enpol.2022.112930.

Monnot, M., Laborie, S., Cabassud, C., 2016. Granular activated carbon filtration plus ultrafiltration as a pretreatment to seawater desalination lines: impact on water quality and UF fouling. Desalination 383, 1–11. https://doi.org/10.1016/j.desal.2015.12.010.

Oka, P.A., Khadem, N., Bérubé, P.R., 2017. Operation of passive membrane systems for drinking water treatment. Water Res. 115, 287–296. https://doi.org/10.1016/j.watres.2017.02.065.

Park, J.W., Kim, H.-C., Meyer, A.S., Kim, S., Maeng, S.K., 2016. Influences of NOM composition and bacteriological characteristics on biological stability in a full-scale drinking water treatment plant. Chemosphere 160, 189–198. https://doi.org/10.1016/j.chemosphere.2016.06.079.

Peter-Varbanets, M., Hammes, F., Vital, M., Pronk, W., 2010. Stabilization of flux during dead-end ultra-low pressure ultrafiltration. Water Res. 44, 3607–3616. https://doi.org/10.1016/j.watres.2010.04.020.

Pronk, W., Ding, A., Morgenroth, E., Derlon, N., Desmond, P., Burkhardt, M., Wu, B., Fane, A.G., 2019. Gravity-driven membrane filtration for water and wastewater treatment: a review. Water Res. 149, 553–565. https://doi.org/10.1016/j.watres.2018.11.062.

Ranieri, L., Putri, R.E., Farhat, N., Vrouwenvelder, J.S., Fortunato, L., 2023. Gravity-driven membrane as seawater desalination pretreatment: understanding the role of membrane biofilm on water production and AOC removal. Desalination 549, 116353. https://doi.org/10.1016/j.desal.2022.116353.

Regula, C., Carretier, E., Wyart, Y., Gésan-Guiziou, G., Vincent, A., Boudot, D., Moulin, P., 2014. Chemical cleaning/disinfection and ageing of organic UF membranes: a review. Water Res. 56, 325–365. https://doi.org/10.1016/j.watres.2014.02.050.

Regula, C., Carretier, E., Wyart, Y., Sergent, M., Gésan-Guiziou, G., Ferry, D., Vincent, A., Boudot, D., Moulin, P., 2013. Ageing of ultrafiltration membranes in contact with

sodium hypochlorite and commercial oxidant: experimental designs as a new ageing protocol. Sep. Purif. Technol. 103, 119–138. https://doi.org/10.1016/j.seppur.2012.10.010.
Robinson, S., Abdullah, S.Z., Bérubé, P., Le-Clech, P., 2016. Ageing of membranes for water treatment: linking changes to performance. J. Memb. Sci. 503, 177–187. https://doi.org/10.1016/j.memsci.2015.12.033.
Robinson, S.J., Bérubé, P.R., 2021. Seeking realistic membrane ageing at bench-scale. J. Memb. Sci. 618, 118606 https://doi.org/10.1016/j.memsci.2020.118606.
Santos, C., Taveira-Pinto, F., Pereira, D., Matos, C., 2021. Analysis of the water–energy nexus of treated wastewater reuse at a municipal scale. Water (Basel) 13, 1911. https://doi.org/10.3390/w13141911.
Senán-Salinas, J., García-Pacheco, R., Landaburu-Aguirre, J., García-Calvo, E., 2019. Recycling of end-of-life reverse osmosis membranes: comparative LCA and cost-effectiveness analysis at pilot scale. Resour., Conserv. Recycl. 150, 104423 https://doi.org/10.1016/j.resconrec.2019.104423.
Shao, S., Wang, Y., Shi, D., Zhang, X., Tang, C.Y., Liu, Z., Li, J., 2018. Biofouling in ultrafiltration process for drinking water treatment and its control by chlorinated-water and pure water backwashing. Sci. Total Environ. 644, 306–314. https://doi.org/10.1016/j.scitotenv.2018.06.220.
Stoffel, D., Rigo, E., Derlon, N., Staaks, C., Heijnen, M., Morgenroth, E., Jacquin, C., 2022. Low maintenance gravity-driven membrane filtration using hollow fibers: effect of reducing space for biofilm growth and control strategies on permeate flux. Sci. Total Environ. 811, 152307 https://doi.org/10.1016/j.scitotenv.2021.152307.
Thaler, P., Hofmann, B., 2022. The impossible energy trinity: energy security, sustainability, and sovereignty in cross-border electricity systems. Polit. Geogr. 94, 102579 https://doi.org/10.1016/j.polgeo.2021.102579.
Turner, S.W., Voisin, N., Nelson, K.D., Tidwell, V.C., 2022. Drought Impacts on Hydroelectric Power Generation in the Western United States (No. PNNL-33212). Pacific Northwest National Lab. (PNNL), Richland, WA (United States). https://doi.org/10.2172/1887470.
Verrecht, B., Maere, T., Nopens, I., Brepols, C., Judd, S., 2010. The cost of a large-scale hollow fibre MBR. Water Res. 44, 5274–5283. https://doi.org/10.1016/j.watres.2010.06.054.
Wu, B., Christen, T., Tan, H.S., Hochstrasser, F., Suwarno, S.R., Liu, X., Chong, T.H., Burkhardt, M., Pronk, W., Fane, A.G., 2017. Improved performance of gravity-driven membrane filtration for seawater pretreatment: implications of membrane module configuration. Water Res. 114, 59–68. https://doi.org/10.1016/j.watres.2017.02.022.
Wu, B., Soon, G.Q.Y., Chong, T.H., 2019. Recycling rainwater by submerged gravity-driven membrane (GDM) reactors: effect of hydraulic retention time and periodic backwash. Sci. Total Environ. 654, 10–18. https://doi.org/10.1016/j.scitotenv.2018.11.068.
Yin, Z., Wen, T., Li, Y., Li, A., Long, C., 2020. Alleviating reverse osmosis membrane fouling caused by biopolymers using pre-ozonation. J. Memb. Sci. 595, 117546 https://doi.org/10.1016/j.memsci.2019.117546.
Zheng, X., Khan, M.T., Croué, J.-P., 2014. Contribution of effluent organic matter (EfOM) to ultrafiltration (UF) membrane fouling: isolation, characterization, and fouling effect of EfOM fractions. Water Res. 65, 414–424. https://doi.org/10.1016/j.watres.2014.07.039.
Zondervan, E., Roffel, B., 2008. Modeling and optimization of membrane lifetime in dead-end ultra filtration. J. Memb. Sci. 322, 46–51. https://doi.org/10.1016/j.memsci.2008.05.023.